

**DESIGN OF COMPOSITES USING FAILURE-MODE-
CONCEPT — BASED TOOLS FROM FAILURE MODEL
VALIDATION TO DESIGN VERIFICATION**

R. Cuntze*

Keywords: structural mechanics building, general material modeling, failure criteria

Novel simulation-driven product development shifts the role of physical testing to virtual testing. This requires High Fidelity concerning material models such as strength failure conditions (SFCs) (strength criteria). Usual assumption for the material model is an ideally homogeneous, usually homogenized solid material. Following Beltrami and Mohr–Coulomb the material element may experience — related to different energy portions — a shape change, a volume change, and friction, and these features can be linked to invariants, which is of great advantage when developing strength criteria. Based on this, the author derived SFCs for a large variety of isotropic brittle structural materials such as plexiglass, porous concrete stone, cast iron, Normal Concrete, UHPC, sandstone, mild steels, foam, monolithic ceramics, further for different transversely-isotropic fiber-reinforced dense and porous polymer UD Laminas (plies, lamellas) and for orthotropic Fabrics such as ceramics. Beside the uniaxial strengths, available multiaxial fracture test data for the materials above-mentioned had to be investigated because in the case of brittle materials these are required to really achieve a 3D-validation of the respective SFC material model. During the development of the Failure Mode Concept FMC, a closer look at material symmetry facts was taken whereby the question arose in the case of ideally homogeneous materials: Is there a ‘generic’ number natural to a material? Namely, Material Symmetry seems to confirm for isotropic materials that this is valid for elastic entities, yield modes and strength fracture modes, for fracture strengths R^t with R^c , fracture toughness entities $K_{Ic} \equiv K_{cr}^t$ with K_{cr}^c and also for the ‘basic’ invariants used to generate SFCs, which usually represent failure, just for the case where the failure mode occurs once. The author concluded from Material symmetry and behavior: (1) ‘Generic Numbers’ exist with a number 2 for isotropic and 5 for UD materials. (2) Different but similar behaving materials can be basically treated with the same SFC.

Retired from industry, MAN-Technologie, Augsburg, German

*Corresponding author; tel.: +49 8136 7754; e-mail: Ralf_Cuntze@t-online.de

Original article submitted February xx, 202x; revision submitted April cc, 202x.

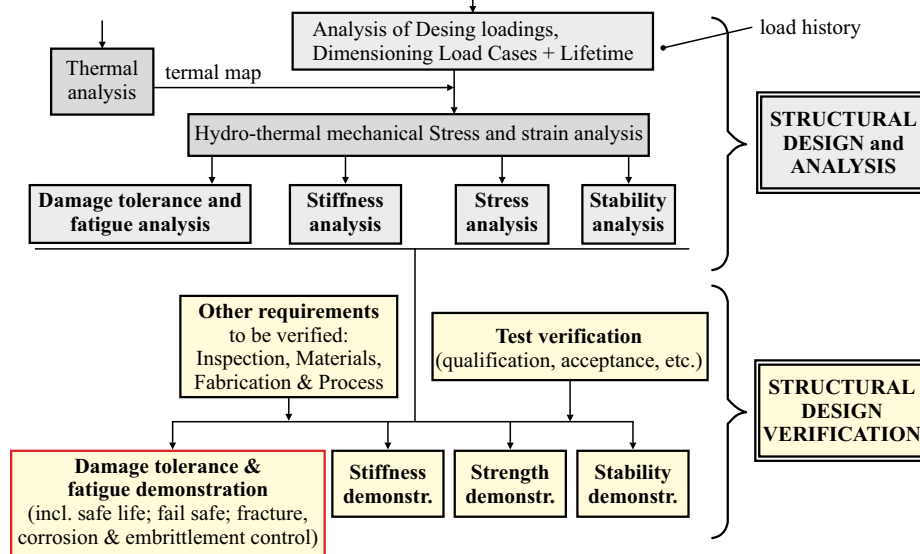


Fig. 1. Structural engineer's tasks and workflow in design.

1. General on Design

The variety of new materials in engineering needs much knowledge about the failure state in order to enable verification of the designed structural part. And this much more since lightweight design requires a higher exertion of the material and thereby contributes to sustainable engineering.

Design Verification demands for reliable reserve factors (RF) and these — beside a reliable structural analysis — demand for reliable SFCs. Such a SFC is the mathematical formulation $F = 1$ of a failure curve or of a failure surface (body). Generally required are a yield condition and fracture strength conditions. A yield SFC usually describes just one mode, i.e. for isotropic materials the classical 'Mises' describes shear yielding (SY). Fracture SFCs usually must describe two independent fracture modes, shear fracture (SF) and normal fracture (NF).

Figure 1 displays the structural engineer's tasks, which he is involved when designing a structural part. Generally, in design verification it is to demonstrate that "No relevant limit failure state is met considering all Dimensioning Load Cases (DLCs)." This involves static DLCs, dynamic and cyclic ones, considering lifetime, and other requirements. Addressed are Design Dimensioning and Design Verification, sometimes termed design proof. Focused on design are the strength design verification of non-cracked structural parts and the fracture mechanics-based design verification of cracked structural parts by Damage Tolerance Tools, see [1].

The size of the damage decides whether it is to apply a SFC with $F = 1$ for the verification of onset-of-fracture in a critical material Hot Spot of the uncracked (*however probably micro-damaged*) structural part or a fracture mechanics-based Damage Tolerance Condition in case of a technical crack (*macro-damaged*).

Design verification with respect to Static Strength shall be performed here on material level by stresses in the critical location of undisturbed areas such as uniform material areas, membrane areas etc. The assessment of the stress states at critical locations captures, using the FMC-based SFCs, the families (*materials are generally composites = a combination of different constituent materials*):

- isotropic material (concrete, glass, etc.),
- transversely-isotropic material (UD = unidirectional material),
- orthotropic (rhombically-isotropic) material (textiles etc.).

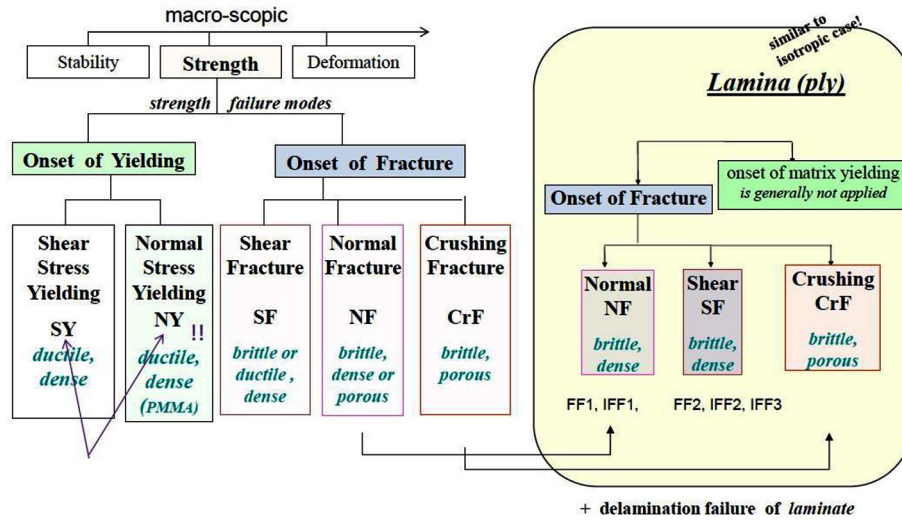


Fig. 2. Proposed scheme of macroscopic strength failure modes of isotropic materials and transversely-isotropic UD-materials (Cuntze1998).

Principally, in order to avoid either to be too conservative or too non-conservative, a separation is required of the always needed ‘analysis of the average structural behavior’ in Design Dimensioning (*using average properties and average stress-strain curves*) in order to obtain best information (= 50% expectation value) from the finally mandatory single Design Verification analysis of the final design, where statistically minimum values for strength and minimum, mean or maximum values for the task-demanded other properties are applied as Design Values.

Statically indeterminate structures are redundant and thereby less risky. In consequence, these are treated differently to the statically determinate ones, which possess just one load path.

2. Scheme of Strength Failure Conditions with Some Definitions

2.1. Scheme of SFCs

In the general development of structural parts, the application of 3D-validated SFCs is one essential pre-condition for achieving the required fidelity for the user. This includes a Yield Failure Condition (ductile behavior) for nonlinear analysis of the material and for design verification at the limit state ‘Onset-of-Yield’. It further includes conditions to verify that ‘Onset-of-Fracture’ does not occur, in the case of both brittle and ductile behavior.

For two decades, the author believes in a macroscopically-phenomenological ‘complete classification’ system, where all strength failure types are included, see Fig. 2 and [2, 3]. In his assumed system, several relationships may be recognized: (1) Shear stress yielding (SY), followed by Shear fracture (SF) considering ‘dense’ materials. For porous materials under compression, the SF for dense materials is replaced by Crushing Fracture (CrF). (2) In order to complete a mechanical system, beside SY also NY should exist. This could be demonstrated by PMMA (plexiglass) with its chain-based texture showing NY due to crazing failure under tension and SY in the compression domain, [1]. The right side of the scheme outlines that a full similarity of the ‘simpler’ isotropic materials with the transversely-isotropic UD materials exists.

Desired as models are *homogeneous* solids; however, reality is much more complicated: Practically, all materials are composites. Structural composites can be metallic, non-metallic or a hybrid combination thereof. One distinguishes two structural composite types: Material Composites and Composite Materials. A structural material usually is the model on the considered scale of a homogenized complex solid that became ‘smeared’ to usually obtain an engineering-like macro-model. A Material Composite is structural-mechanically a composite ‘construction of different materials’ whereas a Composite Material is a combination of constituent materials, different in composition (*constituents retain their identities in the composite; that is, they do not dissolve or otherwise merge completely into each other although they commonly act*). Usually, a composite material can be modeled as smeared material. A not smearable conglomerate such as i.e. carbon fiber grid-reinforced concrete is not a ‘composite material’ despite it is usually termed so.

Some terms for a better common understanding shall be added here: Failure condition: Condition on which a failure becomes effective, meaning $F = 1$ for one limit state. Failure criterion: Distinctive feature defined as a condition for one of the 3 states $F <, =, \text{ or } > 1$. Layer: Physical element from winding, tape-laying process etc. Lamina: Designation of the single UD ply as computational element of the laminate, used as laminate subset or building block for modeling. It might capture several equal plies. First-Ply-Failure (FPF): First Inter-Fiber-Failure (IFF) in a lamina of the laminate. Stress components: They should exactly read stress tensor components or very simple just stresses (*only a shear stress can be composed of a tensile component jointly acting with a compressive stress component*). Simulation: Process, that consists of several analysis loops and lasts until the system is imitated in the Design Dimensioning process. The model parameters are adjusted hereby to the ‘real world’ parameter set. Analysis: Computation that uses fixed model parameters.

3. Basic Knowledge from Former Investigators for the Establishment of SFCs

3.1. Beneficial use of invariants

The Hypothesis of Beltrami for isotropic materials states: “At onset-of-failure (*Beltrami said yielding*) the strain energy density W in a solid material element consists of two portions, one describes the strain energy due to a change in volume (dilatation) and the other the strain energy due to a change in shape (distortion)”. Hence, following Beltrami each invariant term or a multiple of it in the strength failure function F , may be dedicated to one physical mechanism in the solid. Further, these mechanisms are linked to energies, namely $I_1^2 \sim$ dilatational energy from a volume change and $J_2 \sim$ distortional energy from a shape change caused by shear distortion under volume consistency, which was described by Hencky–Mises–Huber (HMH). In the above context, two modeling aspects are to mention:

1. If a material element can be homogenized to an ideal crystal (= *frictionless*), material symmetry requires for the isotropic and the transversely-isotropic UD material a distinct minimum number of properties. This is witnessed by tests.

2. A real solid material model is represented by a description of the ideal crystal + a description of its friction behavior. Mohr-Coulomb asks for the real crystal another physical parameter, namely the inherent material friction value μ with one value for isotropic and two values for UD materials.

Invariants are a combination of stresses — powered or not powered — the value of which does not change when altering the coordinate system (CoS). This attribute is used when looking for an optimum formulation of a usually desired scalar SFC and is valid for UD-materials, too. Figure 3 displays for two material families the dedicated, physically-based choice of invariants.

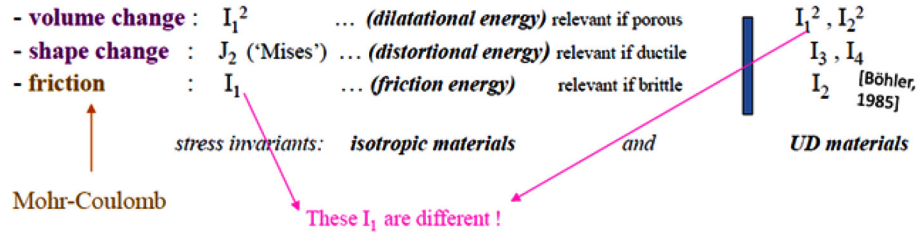


Fig. 3. Choosing invariants when generating SFCs.

3.2. Material symmetry and ‘generic’ number

Under the design-simplifying presumption “Homogeneity is a permitted assessment for the material concerned,” and regarding the respective material tensors, it follows from material symmetry that the number of strengths equals the number of elasticity properties!

Fracture morphology gives further evidence: Each strength property corresponds to a distinct strength failure mode and to a distinct strength failure type, to Normal Fracture (NF) or to Shear Fracture (SF). This means, a characteristic number of quantities is fixed: 2 for isotropic material and 5 for the transversely-isotropic UD lamina (\equiv lamellas in civil engineering). Hence, *the applicability of material symmetry involves that in general just a minimum number of properties needs to be measured* (cost + time benefits) which is helpful when setting up strength test programs. This is beneficial regarding material modeling and the amount of testing. See the literature of Christensen [4].

Witnessed material symmetry knowledge seems to tell: There might exist a ‘generic’ (*term was chosen by the author*) material inherent number for:

Isotropic Material: of 2

- 2 elastic ‘constants’, 2 strengths, 2 strength failure modes fracture (NF with SF) and 2 fracture mechanics modes, which are defined as modes, where the crack plane does not turn

- 1 physical parameter (such as the coefficient of thermal expansion CTE, the coefficient of moisture expansion CME, and the friction value μ , etc.)

Transversely-Isotropic Material: of 5 for the these basically brittle materials

- 5 elastic ‘constants’, 5 strengths, 5 strength failure modes fracture (NFs with SFs)

- 2 physical parameters (CTE, CME, μ ??, etc.).

Since Rolands has basically worked on fiber-reinforced-composites, the author now mainly dedicates his FMC-application to the transversely-isotropic UD-material family.

3.3. Modal and global SFCs

The HMH yield failure condition is a modal SFC that captures just one failure mode. The author chooses the term “global” as a ‘play on words’ to “modal” and to being self-explaining.

Present SFCs can be basically separated into two groups, global and modal SFC ones. Figure 4 presents the main differences between them. Global SFCs describe the full failure surface by one single mathematical equation. This means that for instance a change of the UD tensile strength \bar{R}'_1 affects the failure curve in the *compression* domain, where no physical impact can be! In this context, the modal Tsai-Wu SFC ([5], *responsible parameter* F_{12}) can mathematically not

All modes are married in the Global formulation.
Any change hits all mode domains NF and SF of the fracture body surface

Drucker-Prager, Ottosen, Willam-Warnke, Tsai-Wu,
Altenbach/Bolchun/ Kulupaev, Yu , etc.

1 Global SFC :	$F(\{\sigma\}, \{R\}) = 1$	global formulation, usually
Set of Modal SFCs :	$F(\{\sigma\}, \{R^{\text{mode}}\}) = 1$	model formulation in the FMC

Mises,Puck,Cuntze

All modes are separately formulated.
Any change hits only the relevant domain of the fracture body surface

$F(\{\sigma\}, \{R^{\text{mode}}, \mu^{\text{mode}}\}) = 1$	more precise formulation
---	--------------------------

by direct introduction of the friction value
considering Mohr-Coulomb for brittle materials under compression

$$UD : \quad \{\sigma\} = (\sigma_1, \sigma_2, \sigma_3, \tau_{23}, \tau_{31}, \tau_{21})^T, \quad \{\bar{R}\} = (\bar{R}'_{||}, \bar{R}^c_{||}, \bar{R}'_{\perp}, \bar{R}^c_{\perp}, \bar{R}_{||}, \bar{R}_{\perp}; \mu_{||}, \mu_{\perp})^T$$

$$Isotrop : \quad \{\sigma\} = (\sigma_x, \sigma_y, \sigma_z, \tau_{yz}, \tau_{zx}, \tau_{xy})^T = (\sigma_I, \sigma_{II}, \sigma_{III})^T, \quad \{\bar{R}\} = (\bar{R}', \bar{R}^c; \mu)^T$$

Needs an interaction of Failure Modes:

This is performed by a probabilistic approach (series failure system) in the transition zones between neighboring modes NF and SF

Fig. 4. ‘Global’ and ‘modal’ SFCs.

really map the failure curve $\sigma_2(\sigma_1)$ of WWFE-I, TC3, [1, 6-10] in the compression domain as test data of the IKV Aachen is demonstrating [1, Kopp]. Hence, the computed *Reserve Factor* may not be on the safe side in this domain.

Often, SFCs employ just strengths and no friction value. This is physically not accurate. Mohr–Coulomb acts in the case of compressed brittle materials! The undesired consequence in Design Verification again is: The computed *Reserve Factor* may be not on the safe side.

4. Features of the Failure-Mode-Concept and the UD SFCs Derived from

4.1. Basic features

The basic features of the FMC, derived about 1995, are the following [1, 2, 11, 12].

- Each failure mode represents 1 independent failure mechanism and thereby represents 1 piece of the complete failure surface.
- A failure mechanism at the lower microscopic mode level shall be considered in the applied desired macroscopic SFC.
- Each failure mechanism or mode is governed by 1 basic strength R , only (*witnessed!*).
- Each failure mode can be represented by 1 SFC.

Therefore, equivalent stresses can be computed for each mode. This is of advantage when deriving $S - N$ curves and generating Haigh diagrams in fatigue with minimum test effort in order to relatively effortless obtain Constant Fatigue Life curves, see [1] for lifetime estimation. Modal SFCs lead to a clear mode strength-associated equivalent stress.

TABLE 1. ‘Dense’ UD materials: SFC Formulations for FF1, FF2 and IFF1, IFF2, IFF3

Column Name???
FF1: $Eff^{\parallel\sigma} = \bar{\sigma}_1 / \bar{R}'_{\parallel} = \sigma_{eq}^{\parallel\sigma} / \bar{R}'_{\parallel}$ with $\bar{\sigma}_1 \cong \varepsilon_1^t \cdot E_{\parallel}$ (matrix neglected)
FF2: $Eff^{\parallel\tau} = -\bar{\sigma}_1 / \bar{R}'_{\parallel} = +\sigma_{eq}^{\parallel\tau} / \bar{R}'_{\parallel}$ with $\bar{\sigma}_1 \cong \varepsilon_1^c \cdot E_{\parallel}$
IFF1: $Eff^{\perp\sigma} = [(\sigma_2 + \sigma_3) + \sqrt{\sigma_2^2 - 2\sigma_2 \cdot \sigma_3 + \sigma_3^2 + 4\tau_{23}^2}] / 2\bar{R}'_{\perp} = \sigma_{eq}^{\perp\sigma} / \bar{R}'_{\perp}$
IFF2: $Eff^{\perp\tau} = [a_{\perp\perp} \cdot (\sigma_2 + \sigma_3) + b_{\perp\perp} \sqrt{\sigma_2^2 - 2\sigma_2 \sigma_3 + \sigma_3^2 + 4\tau_{23}^2}] / \bar{R}'_{\perp} = \sigma_{eq}^{\perp\tau} / \bar{R}'_{\perp}$
IFF3: $Eff^{\perp\parallel} = \{[b_{\perp\parallel} \cdot I_{23-5} + (\sqrt{b_{\perp\parallel}^2 \cdot I_{23-5}^2 + 4 \cdot \bar{R}'_{\perp}^2 \cdot (\tau_{31}^2 + \tau_{21}^2)^2}] / (2 \cdot \bar{R}'_{\perp}^3)\}^{0.5} = \sigma_{eq}^{\perp\parallel} / \bar{R}'_{\perp\parallel}$
$\{\sigma_{eq}^{\text{mode}}\} = (\sigma_{eq}^{\parallel\sigma}, \sigma_{eq}^{\parallel\tau}, \sigma_{eq}^{\perp\sigma}, \sigma_{eq}^{\perp\tau}, \sigma_{eq}^{\perp\parallel})^T$, $I_{23-5} = 2\sigma_2 \cdot \tau_{21}^2 + 2\sigma_3 \cdot \tau_{31}^2 + 4\tau_{23}\tau_{31}\tau_{21}$
Inserting the compressive strength point $(0, -\bar{R}'_{\perp}) \rightarrow a_{\perp\perp} \cong \mu_{\perp\perp} / (1 - \mu_{\perp\perp})$, $b_{\perp\perp} = a_{\perp\perp} + 1$ from a measured fracture angle $\rightarrow \mu_{\perp\perp} = \cos(2 \cdot \theta_{fp}^{\circ} \cdot \pi / 180)$, for $50^{\circ} \rightarrow \mu = 0.174$. $b_{\perp\parallel} \cong 2 \cdot \mu_{\perp\parallel}$. Typical friction value ranges: $0 < \mu_{\perp\parallel} < 0.25$, $0 < \mu_{\perp\perp} < 0.2$.

- Of course, a modal FMC-approach requires an interaction in all the mode transition zones reading

$$Eff = \sqrt[m]{(Eff^{\text{mode } 1})^m + (Eff^{\text{mode } 2})^m + \dots} = 1 = 100\% \text{ for Onset-of-Failure.}$$

It employs the so-called ‘material stressing effort’ (*artificial term, generated in the WWFE in order to get an English term for the excellent, meaningful German term Werkstoffanstrengung*) analogous to ‘Mises’

$$Eff^{\text{yield mode}} = \sigma_{eq}^{\text{Mises}} / R_{0.2} \rightarrow Eff^{\text{fracture mode}} = \sigma_{eq}^{\text{fracture mode}} / R$$

with a mode interaction exponent m , also termed rounding-off exponent, the size of which is high in case of low scatter and vice versa. The value of m is obtained by curve fitting of test data in the transition zone of the interacting modes. General FRP mapping experience delivered that $2.5 < m < 3$. A lower value chosen for the interaction exponent is more on the safe RF side or more ‘design verification conservative.’ For CFRP, $m = 2.6$ is recommended from mapping experience. From engineering reasons, the interaction exponent m is chosen the same in all transition zones of adjacent mode domains. Using the interaction equation in the mode transition zones is leading again to a pseudo-global failure curve or surface. In other words, a ‘single surface failure description’ is achieved again, such as with Tsai–Wu but without the shortcomings of the global SFCs.

Above interaction of adjacent failure modes is modeled by the ‘series failure system’. That permits to formulate the total material stressing effort Eff generated by all activated failure modes as ‘accumulation’ of $Eff^{\text{modes}} \equiv$ sum of the single mode failure danger proportions. $Eff = 100\% = 1$ represents the mathematical description of the complete surface of the failure body! In practice, i.e., in thin UD laminas, at maximum, 3 modes of the 5 modes (2 FF + 3 IFF) will physically interact. Considering 3D-loaded thick laminas embedded in laminates, there, all 3 IFF modes might interact.

4.2. Cuntze’s FMC-based SFCs

Of interest is not only the interaction of the fracture surface portions in a *mixed failure domain* or transition zone of adjacent failure modes, respectively, but failure in a *multi-fold failure domain* (superscript ^{MIFD}) such as in the (σ_2^t, σ_3^t) -domain. There the associated mode material stressing effort acts twofold. It activates failure in two orthogonal directions

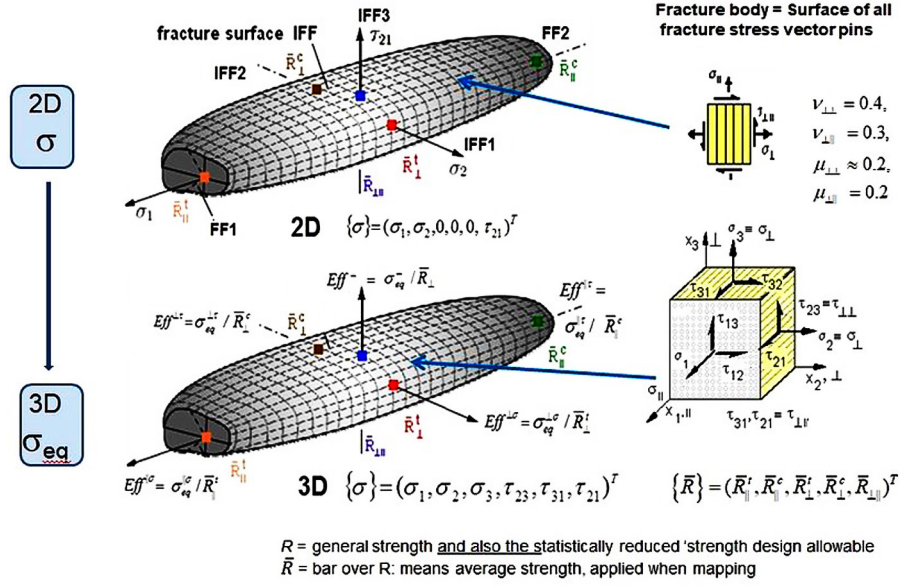


Fig. 5. From a 2D failure body to a 3D failure body by replacing stresses by equivalent stresses.

which may be considered by adding a multi-fold failure term, proposed in [13] for isotropic materials. It can be applied as well to brittle UD-material in the quasi-isotropic transversal plane $\sigma_2(\sigma_3)$.

Table 1 collects the FMC-derived 5 SFC formulations. The applied invariants

$$I_1 = \sigma_1, \quad I_2 = \sigma_2 + \sigma_3, \quad I_3 = \tau_{31}^2 + \tau_{21}^2, \quad I_4 = (\sigma_2 - \sigma_3)^2 + 4 \cdot \tau_{23}^2,$$

$$I_5 = (\sigma_2 - \sigma_3) \cdot (\tau_{31}^2 - \tau_{21}^2) - 4\tau_{23}\tau_{31}\tau_{21},$$

stem from [14].

'Porous' UD material [1]: Replacement of IFF2 by using

$$Eff_{porosity}^{SF} = \sqrt{a_{\perp\perp por}^2 \cdot I_2^2 + b_{\perp\perp por}^2 \cdot I_4 - a_{\perp\perp por} \cdot I_2} / 2\bar{R}_{\perp}^c.$$

From friction parameters b to friction values μ : The structural stresses-formulated UD-fracture curve $\sigma_2(\sigma_3)$ could be transferred into a Mohr-Coulomb one obtaining $\tau_{nt}(\sigma_n)$ [1]. This novel, mathematically pretty effortful transformation enabled the author to link the fictitious friction parameters b of the respective SFCs via a determined fracture angle with the measurable physical friction value μ , see also [15].

Figure 5 depicts the failure body of UD materials. The upper picture contains the failure body of the 2D plane stress state and the lower picture the body of the 3D stress state. These look the same and are the same. One must only replace the UD-lamina stresses of the 2D-case by equivalent stresses to obtain the 3D-fracture failure body.

Delamination within a laminate may occur in tensile-shear and compression-shear cases (*remember the so-called wedge failure of Puck with its inclined fracture plane [9]*). Considering such a delamination a 3D stress state is to be regarded. This is especially the case if bends in the structure are tensioned or compressed which generates stresses across the wall thickness. These stresses are activated by the delamination-critical interlaminar stress state

$$\{\sigma\}_{lamina} = (0, \sigma_2, \sigma_2, \sigma_3, \tau_{23}, \tau_{31}, \tau_{21})^T.$$

Before introducing the UD-SFC, some prerequisites are to verify that a *reliable design* process is actually achieved before applying the SFC. This is valid for test specimens, as well:

- Good fiber placement and alignment, and uniform distribution.
- ‘*Fabrication signatures*’ such as fabrication-induced fiber waviness and wrinkles are small and do not vary in the test specimens.
- If applicable, residual stresses from the curing cycle are to be computed for the difference ‘*stress free temperature to room temperature 22°C*’ as an effective temperature difference. Considering curing stresses or moisture stresses, the specimens are most often assumed to be well conditioned.
- The stress-strain curves are average curves in design dimensioning, which is also the type one needs for test data mapping in order to obtain the best estimation, namely 50%.

5. Application of Static UD SFCs to Test Results in WWFE-I and II

Referring to the WWFE: At first, 1000 thanks to the WWFE-organizers from QinetiQ in the UK namely to Mike, Sam, Peter and later Shuguang for setting up such long-lasting effortful World-Wide Failure Exercises (WWFE) with its origin in 1992. I am very grateful for your huge effort, especially to Sam despite of my later following critics: We contributors know that you could only provide us with available test data sets, where the quality of them was not fully known. But, we contributors should have commonly discussed with you your test data input. There was one TestCase-example, only.

To understand the WWFE procedure, the following information is necessary for the reader.

— Part A, blind prediction: This was to perform without provision of all needed properties, for example, with strength values alone. In general, a validated SFC cannot be applied in case of lacking friction information. For compression test cases, a friction value μ or a fracture information about it should have been given. *How is a comparison between SFCs of the contributors possible if the necessary data basis is not complete and partly not sound?*

— Part B, comparison Theory-Test: Strength values have been changed on occasion with Part B, some test data sets were partly not applicable and even false failure points were involved. *Missing information that should have been provided for the blind prediction was sometimes firstly available in Part B, too late for Part A.*

5.1. Static validation of the UD failure criteria (material models) on UD laminas

There are three WWFEs that have been executed since 1992: WWFE-I for testing strength fracture criteria by checking the mapping quality of 2D-fracture stress states of the lamina. Then, WWFE-II for 3D-fracture stress states (*see the later body text*) for achieving 3D-lamina model validation and laminate.

After all, it was intended to test (Micro)Damage Models based on Continuum-(Micro)Damage-Mechanics theory in WWFE-III to the full. However, a final result is not yet available.

The author did not participate in WWFE-III but would like to give some comments as industrial user with some experience in this field (see, Ch. 1 in [1]). One essential aim of the micro-damage models for ductile and brittle behaving materials is to gain more knowledge about the local failure situation. Therefore, a mesoscale is employed which — in UD context — structural engineers define to lie between micro- and macro-scales (*for polymer engineers meso is factor thousand lower!*), which are the official scales.

In Design Dimensioning, one can clearly determine a model parameter set that describes the average behavior well and fits the structural test results. Sometimes, after a simulation process that requires the performance of many analyses in

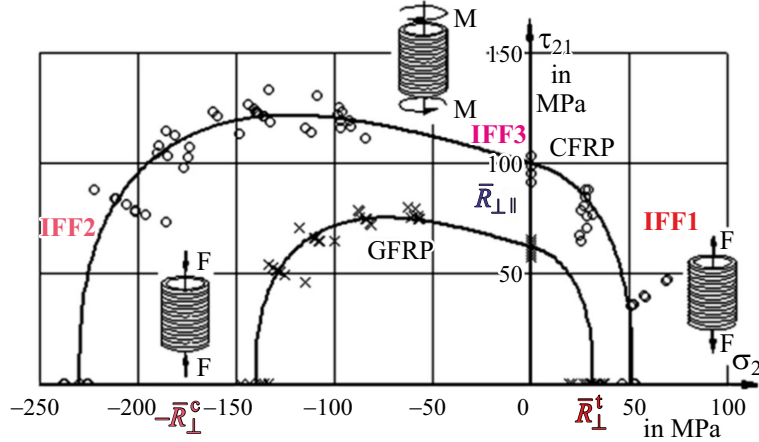


Fig. 6. IFF test results: 2 GFRP, 1 CFRP Test Series [MAN Technologie project].

order to simulate the component behavior to finally achieve a suitable design parameter set. After some experience, this enables to build a prototype but not to build safety-critical structural parts, which must be design-verified. For these parts, in Design Verification a statistically based approach with a minimum number of measurable design parameters is mandatory. Classically, a Safety Concept is given with Design Factors of Safety j or γ based on long-term experience and finally a positive Reserve Factor (RF) is to demonstrate. Using micro-damage mechanics models – analogous, to determine RF – statistically-based micro-damage model input parameters are required and a maximum value D is to define following

$$D < D_{admissible} \text{ (should be statistically based)} < 1 \text{ at failure.}$$

Defining the D — value is a challenge for the application of (Micro)Damage Models for serial production certification. It is higher than for strength design allowables R .

Coming back: WWFE-I and WWFE-II intended to “test the contributor’s ‘failure theory’ to the full,” whereby the WWFE ‘failure theory’ involved 3 elements: The SFCs, the numerical procedure such as a FE code, and the nonlinear analysis tools. This confuses the user because he just looks for a reliable macro-mechanical SFC that hopefully captures on top generated microscopic failures by the proposed SFC equations for the UD-lamina. The author’s FF1- and FF2-formulations, for instance, take care, that transversal equi-biaxial compression might cause FF1.

The normal user is just interested to well map his course of failure test data by an SFC. Exemplarily in Fig. 6, for the partly model-validation $\tau_{21}^{fr}(\sigma_2)$, the basic cross-section of the failure body, an own 2D-fracture stress data set from a ‘tension/compression-torsion test machine’ is displayed.

5.2. Investigation and assessment of some WWFE-test cases (TC)

Validation of the lamina-material SFCs models can be only achieved by 2D- together with 3D-lamina test results. Since SFC-model validation is focused, just lamina-TCs are now investigated in detail.

The laminata test cases serve for the verification of the laminate design. There, the full WWFE failure theory is required. This makes a comparison between the contributions very challenging because different FE codes were applied by the contributing competing institutes. These better tools further had to be equally compared to the retired author’s tools, who could just use his handmade nonlinear CLT-code upgraded by experience and sensibleness for the problem and the delivered input.

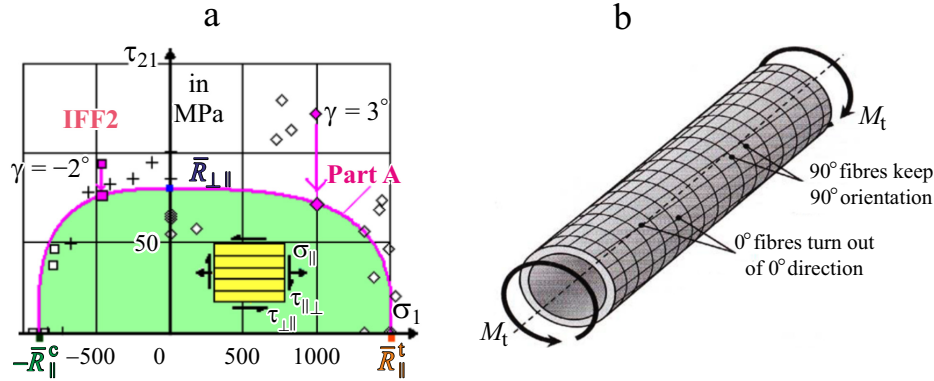


Fig. 7. (a) WWFE-I, TC2, UD lamina, CFRP, T300/BSL914C Ep, $\tau_{21}^{fr}(\sigma_1)$, (b) Tube test specimen picture: [Courtesy IKV Aachen].

Of high interest for future scientists and engineers might be the following Lessons Learned (LL) of the author during his many WWFE-designated years. They are the result stemming from a very careful and effortful test data evaluation of about one-man year spent by the author. Otherwise, a successful contribution would not have been made possible by the author. Thereby, some essential examples for lamina input shortcomings are found.

- WWFE-I, TC1: the strengths provided have been changed from Part A to B and two test points are doubtful w.r.t. test results of the author, comparing Fig. 6 (*Reason, known by the author: non-accurate raw test data evaluation of the test engineer at DLR Stuttgart*).

- WWFE-I TC2: the author informed the organizers that apples and oranges were put here together in a diagram. One cannot fill into the same diagram 90°-wound tube test specimen data together with 0°-wound tube data. The 0°-stresses have to be transformed in the 2D-plane due to the fact that shearing under torsion loading (see Fig. 7) turns the fiber direction and the lamina coordinate system (CoS) is not anymore identical with the structure coordinate system of the tube. In order to also use these test data, the author exemplarily transformed two fracture test point [16] data by the occurring twisting angle using a nonlinear CLT-analysis. Then, he could achieve a good mapping showing that — in the lamina CoS — the two transformed fracture points accurately lie on the 90°-curve.

- WWFE-II, TC3: the same mistake happened again, but there the much more complicated 3D-stress situation is to face, so that the 3D-transformation of the 0°-data set could not be simply performed, see [1, 16,17].

- WWFE-II, TC2 an average stress-strain curve should have been provided because otherwise no realistic treatment is possible. Therefore, the Part A results could be only inaccurate. From the Part B information, the author could derive an average curve and then all 3 TC test data courses could be mapped and the mutual check points in the fully connected TC2-TC3-TC4 matched. Incomprehensively, there was no response of the organizers to the author's idea, which made 3 TCs to successful test cases.

- Viewing the papers “*A comparison of the predictive capabilities of current failure theories for composite (UD-composed) laminates, judged against experimental evidence*” [18] and “*Maturity of 3D failure criteria for fiber-reinforced composites: Comparison between theories and experiments Part B of WWFE-II*” [19], there is not any doubt to find concerning the quality of the available and provided test data sets. One third of the TCs is at least questionable up to not applicable for a model validation.

SFCs models have shortcomings and these shortcomings can only be reduced by using test data that represent real experimental evidence. Consequently, “What is the real WWFE output? Is there a realistic progress with the SFCs? Part A

practically had no additional value for the industrial user. With Part B, partly a realistic progress could be achieved and this progress were better if the tests data sets would had been commonly interpreted.

Whereas in [18] an assessment of the various SFCs was formulated, this is more or less missing in WWFE-II, Part B. This discourages theoreticians and practitioners and is not acceptable for the industry, which has to design verify structural parts by reliable SFCs. In industry, one person has to sign a Design Verification before production and use. This means to take responsibility for the product. I had thought that WWFE-II would also present a realistic SFC assessment basis for us industrial users.

(Not to forget. Two non-funded German engineers won WWFE-I with their UD-SFCs: Cuntze with his Failure-Mode-Concept based criteria and Puck with his Action Plane criteria).

5.3. Some notes on experience with WWFE-I and -II

1. QinetiQ counted the number of parameters used in each theory: This resulted in the statement “Cuntze needs 75 parameters” which usually leads for a user to “Such a criteria set is not applicable in practice. Forget Cuntze’s FMC-based SFCs.” Above counting was a counting of apples and oranges and showed very clearly the discrepancy “Failure Theory ↔ Failure Criterion”. The reality is: For his set of 5 UD failure criteria Cuntze needs 7 measurable model parameters (5 strengths + 2 friction values) and — from experience — a given interaction exponent m . In this context, it is to mention: Other contributors seem not to know that for a reliable modeling material friction values μ must be used under compression! They only employ the 5 strengths, which means less parameters for the their bottlenecked SFCs. Mohr-Coulomb acts and therefore the use of just 5 strength parameters (*unfortunately supported by the organizers*) is not accurate! It should further be noted: For all those contributors, which did not perform all required tasks, a smaller number of parameters has been counted, naturally too. That looks better, of-course. “Good FMC-Mapping is not the power of 75 parameters” as R. M. Christensen correctly published (reflecting me) however not knowing how the counting was performed.

2. Provided test data sets: An invitation, to speak about error-prone test data, found no response at QinetiQ. In the past and presently, users still apply inaccurate WWFE test data sets for model validation. This is a pity! One cannot validate a hopefully good SFC using false test data, however vice versa, one can check the course of measured test data with a validated SFC.

3. Why did QinetiQ practically require from the contributing transversely-isotropic, physically different macroscopic UD-SFCs that they should capture the isotropic matrix failure behavior, as well?

4. For the isotropic matrix in WWFE-II, TC1 no sufficient information was provided in order to obtain enough knowledge for matrix behavior modeling.

5. Micro-mechanical analysis: Here, QinetiQ provided just micro-mechanical material properties but forgot to provide the contributors with the absolutely necessary associated micro-mechanical relationship. Not surprisingly, the author found a discrepancy of a factor of 2 for the data to be predicted using own micro-mechanical equations that do not belong to the provided fiber and matrix properties, of course! Micro-mechanical formula has to be always given together with the associated micro-mechanical properties.

6. Hydrostatic pressure beyond 200 N/mm² or 200 MPa (1 MPa ≡ 10 bar) changes the polymer behavior. The effect was known at QinetiQ from own tests but no information was provided to feed the necessary model derived by the author in Part A for the TCs experiencing $p_{\text{hyd}} > 200$ MPa. This ‘Birch finite strain modulus increase effect’ [17, 20] characterizes a second glass transition point T_g and was therefore termed by the author 2nd T_g -shift of the matrix material.

7. Lamina properties, used as input for analysis, are test results from *isolated* UD lamina test specimens such as a tensile coupon. They are load-controlled derived and the results are of weakest link type, whereas the in-situ behavior of a UD lamina embedded in a laminate is deformation-controlled and therefore of redundant type. This is to capture in nonlinear laminate analysis after IFF of the first ply in the laminate.

8. Closed and open failure envelopes: The tensile cap is always closed whereas the compressive bottom might be closed or not, porosity leads to a bottom closure. Further, in contrast to an isotropic dense material, at ultra-high hydrostatic pressures (3D) of some thousands MPa the fiber fails by tensile fracture caused by the acting Poisson effect!

9. Delamination is a failure in the 'structure' laminates, and at its edges it is termed edge effect. Within the laminate, it can be predicted by the application of the interlaminar stresses-associated 3D-SFCs. At the edges, it is — due to the stress singularity — a task of fracture mechanics tools using a cohesive zone model.

Test the provided test results, analyze your analysis, it might be cruder than you think. Always use information to improve an investigation.

5.4. Example Design Verification of the critical UD lamina of a distinct wall design

Design Verification requires a Reserve Factor $RF \geq 1.00$. A very simple example shall depict the RF -calculation procedure:

Assumption: Linear analysis permitted, design FoS $j=1.25$

$$*2D\text{-stress state: } \{\sigma\} = (\sigma_1, \sigma_2, \sigma_3, \tau_{23}, \tau_{31}, \tau_{21})^T \quad j = (0, -60, 0, 0, 0, 50)^T$$

*Residual stresses: 0 (effect vanishes with increasing micro-cracking)

$$*\text{Strengths: } \{R\} = (R_{\parallel}^t, R_{\parallel}^c, R_{\perp}^t, R_{\perp}^c, R_{\perp\parallel})^T = (1050, 725, 32, 112, 79)^T \text{ MPa}$$

$$\{\bar{R}\} = (1378, 950, 40, 125, 97)^T \text{ MPa estimated from average values}$$

Friction values: $\mu_{\perp\parallel} = 0.3$, ($\mu_{\perp\perp} = 0.35$), Mode interaction exponent: $m = 2.7$

$$*Eff^{\perp\sigma} = \frac{\sigma_2 - |\sigma_2|^*}{2 \cdot \bar{R}_{\perp}^t} = 0, \quad Eff^{\perp\tau} = \frac{-\sigma_2 + |\sigma_2|}{2 \cdot \bar{R}_{\perp}^c} = 0.60, \quad Eff^{\perp\parallel} = \frac{|\tau_{21}|}{\bar{R}_{\perp\parallel} - \mu_{\perp\parallel} \cdot \sigma_2} = 0.51$$

$$Eff^m = (Eff^{\perp\sigma})^m + (Eff^{\perp\tau})^m + (Eff^{\perp\parallel})^m$$

$$\Rightarrow Eff = 0.72, \quad RF = 1 / Eff = 1.39, \quad MoS = RF - 1 = 0.39 \text{ (must be positive!).}$$

The certification-relevant load-defined Reserve Factor RF corresponds in the linear case to the material reserve factor f_{RF} . Its value here is $1.39 > 1 \rightarrow$ Laminate wall design is verified!

(Note: The purpose of the design FoS j is to guaranty quality of the design in order to achieve a certain level of Structural Reliability for the hardware. Different industry has different risk acceptance attitudes and applies differently high FoS values!)

6. Application of the UD-SFCs to Cyclic Test Results

Basic aim in fatigue design is to reduce the test amount of $S - N$ curves to a minimum. This was a long-lasting task for the author and had to be practically solved.

The FMC-based static SFCs enable to provide a novel life-time prediction method. An analytical, automatic establishment of a continuous Constant Fatigue Life CFL curve $\sigma_a(\sigma_m, N = \text{const})$ — basis of lifetime estimations — could be developed (N is the failure cycle number and n running cycle number). At first, a function for mapping the course of the $S - N$ -curve test data was searched. Chosen was the 4-parameter Weibull curve model. In order to reduce the test amount, a further task was to find a physically-based model to predict other $S - N$ curves, required for fatigue analysis, on basis of probably just one Master $S - N$ curve for each mode. Finally, a challenging task was the very difficult mapping of the *test data falling*

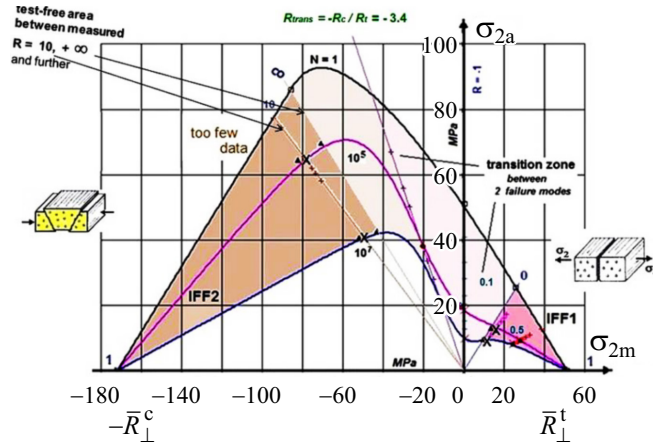


Fig. 8: Example IFF1-IFF2 UD Haigh diagram displaying the failure mode domains, transition zone [data, courtesy Dr.-Ing. Clemens Hahne, AUDI].

in the transition zone where the modes interact around the stress ratio beam $R_{\text{transition}} = -R^c / R^t < R = \min \sigma / \max \sigma = -1$, which lies more right in the Haigh diagram (Fig. 8). This is the most problematic region in the Haigh diagram, especially if the *strength ratio* R^c / R^t is high. A solution became possible by a mode decay function which physically terminates the influence of the SF part (*compression*) in the Haigh diagram when the NF part begins at $R = 0$ and vice versa for the NF part (*tension*), the opposite decay. Essential thereby was that the FMC-based static SFCs are equivalent stress curves of a mode, of SF and of NF. See the Table 2 with the procedure of determining a lifetime Reserve Factor.

6.1. Derivation of a constant fatigue life model and application (example UD)

The derivation considered the following points.

- Assumption: “If the failure mechanism of a mode cyclically remains the same as in the brittle static case, then the micro-damage-driving fatigue failure parameters are the same and the applicability of static SFCs is allowed for quantifying micro-damage portions.”

- Presumption: An appropriate Master $S - N$ curve for each failure mode domain compression (SF) and tension (NF) is available. This means measurement of just a minimum number of $S - N$ curves is necessary.

- The searched helpful model became the ‘Modified Fatigue Strength Ratio Ψ ’ model’ of Masamichi Kawai [21], which enables to estimate the bunch of all measured $S - N$ curves. Cuntze dedicated Ψ to the single failure modes or Haigh domains SF and NF. Other necessary $S - N$ curves, necessary for the verification of the usually faced variable amplitude operational loading, can then be derived from the Master $S - N$ curve [1]. Asymptotic R -curves are automatically captured by the model.

- The model quality in Fig. 8 proves the efficiency of the decay functions in the transition zone, where – in contrast to this example – seldom test data is available. Thanks to C. Hahne [22].

- By the way: The decaying course of the curve in the graph below is similar for UD material and concrete due to their large strength ratios R^c / R^t !

Kawai captures all $S - N$ curves in tension (NF) and in compression (SF) domain by one Ψ and then he determines also $S - N$ curves in the transition zone around R_{trans} . Cuntze separates the mode regimes to stay in the mode domains bet-

TABLE 2. Full Procedure of the Automatic Determination of a Constant Fatigue Life Curve

Column Name???

*Relationships

$$\sigma_{\max} = \Delta\sigma / (1-R) \equiv 2 \cdot \sigma_a / (1-R) \text{ with } \Delta\sigma = \text{stress range, } \sigma_a \text{ is positive}$$

$$R = (\sigma_m - \sigma_a) / (\sigma_m + \sigma_a), \sigma_a = \sigma_m \cdot (1-R) / (1+R)$$

$R = -1$, fully reversed alternating stress. $R = 0$, $R = 100$ (°), extreme swelling stresses.

$$\bar{R}^t = \sigma_{\max} (n = N = 1), \bar{R}^c = \sigma_{\min} (n = N = 1)$$

$$\sigma_a = 0.5 \cdot \sigma_{\max} \cdot (1-R), \sigma_m = 0.5 \cdot \sigma_{\max} \cdot (1+R);$$

$$\sigma_a = -0.5 \cdot \sigma_{\min} \cdot (1-R^{-1}), \sigma_m = \sigma_{\min} (1-0.5 \cdot (1-R^{-1}))$$

*Choice of problem-adequate mapping function and individual mapping of course of test data

$$\sigma_{\max}(N) = c1 + (\bar{R} - c1) / \exp\left(\frac{\log(N)}{c3}\right), \sigma_{\min}(N) = c1 + (-\bar{R} - c1) / \exp\left(\frac{\log(N)}{c3}\right)^{c2}$$

*Test input and mapping available Master curves (usually just available for $r = 0.1$ and 10)

$$\sigma_{R=0.1} = c_1^{NF} + (\bar{R}^t - c_1^{NF}) / \exp\left(\frac{\log(N)}{c_3^{NF}}\right)^{c_2^{NF}}, \sigma_{R=10} = c_1^{SF} + (-\bar{R}^c - c_1^{SF}) / \exp\left(\frac{\log(N)}{c_3^{SF}}\right)^{c_2^{SF}}$$

*Mode dedicated Application of Kawai's model $\Psi = \sigma / \bar{R}$; ψ, Ψ positive

$$\text{Static failure occurs at } \sigma_{\max} = \bar{R}^t = \sigma_a + \sigma_m \text{ and } \sigma_{\min} = -\bar{R}^c = -\sigma_a + \sigma_m.$$

$$\sigma_{\max} = \bar{R}^t = \sigma_a + \sigma_m \rightarrow \sigma_a = \bar{R}^t - \sigma_m \rightarrow 1 = \sigma_a / (\bar{R}^t - \sigma_m) \equiv \text{cyclic / 'static'}$$

*Kawai's cyclic danger intensity to fail ($N > 1$) is given for tension and compression

$$\Psi_{Master}^t = \sigma_a / (\bar{R}^t - \sigma_m) \quad \text{and} \quad \Psi_{Master}^c = \sigma_a / (\bar{R}^t + \sigma_m).$$

*Relationship of available Master curves with Ψ

*Inserting σ_a, σ_m brings the stress ratio R into the model

$$\Psi_{Master}^t = 0.5 \cdot \sigma_{\max}^{Master} \cdot (1-R) / [\bar{R}^t - 0.5 \cdot \sigma_{\max}^{Master} (1+R)]$$

$$\Psi_{Master}^c = \sigma_{\min}^{Master} \cdot (1-R) / [2 \cdot R \cdot \bar{R}^c + \sigma_{\min}^{Master} \cdot (1+R)].$$

*Resolution of above equations for a novel $S-N$ curve or of a CFL curve (inserting σ_a, σ_m)

$$\sigma_{NF\text{domain}} = 2 \cdot \bar{R}^t \cdot \Psi_{Master}^t / (\Psi_{Master}^t - R + R \cdot \Psi_{Master}^t + 1), \quad 0 < R < 1$$

$$\sigma_{SF\text{domain}} = -2 \cdot \bar{R}^c \cdot R \cdot \Psi_{Master}^c / (\Psi_{Master}^c + R + R \cdot \Psi_{Master}^c - 1)$$

$$\sigma_{R=0} = 2 \cdot \bar{R}^t \cdot \Psi_{Master}^t / (\Psi_{Master}^t - 0 + 0 \cdot \Psi_{Master}^t + 1) \quad R = 0$$

$$\sigma_{R=100} = -2 \cdot \bar{R}^c \cdot 100 \cdot \Psi_{Master}^c / (\Psi_{Master}^c + 100 + 100 \cdot \Psi_{Master}^c - 1) \text{ for } R = 100 (\approx \infty)$$

*For information: Decay function

$$f_{\text{decay}} = 1 / (1 + \exp(c1 + \sigma_m / c2)).$$

ter physically-based. However, then he needs above mentioned decay function $f_{\text{decay}} = 1 / (1 + \exp(c1 + \sigma_m / c2))$ in both the domains to make the determination of $S - N$ curves and of CFL curves in the transition zone possible. A quality check of the two approaches is possible if enough $S - N$ curves, distributed over the full Haigh diagram, will be available in literature for a material with a large strength ratio.

The full procedure is collected in the Table 2. Here, and this is reasonable for brittle materials, all the S-N curves have their origin in the strength points \bar{R}^t and \bar{R}^c .

Mind: For $n > 1$, at failure, $Eff = 100\%$ becomes replaced by the micro-damage sum total $D = 100\%$, and the static strength by the cyclic strength as function.

(The associated full MathCad program, that involves test data evaluation, parameter determination of Weibull curves, of Master curves, of decay functions, computation operations and visualization afforded more than 30 pages of a strictly logically built-up procedure).

6.2. Design Verification of a critically cycled UD lamina within a chosen laminate

To be practical, a work case of fatigue life estimation shall be presented. As the employment of the decay function is too lengthy here just two $S - N$ curves in the tension domain are stressed.

Example UD material, IFF1-IFF2: Test data, courtesy C. Hahne, see Fig. 8.

*Given: $\sigma_2 = \sigma_{2a} + \sigma_{2m}$, $\bar{R}_\perp^t = 51$ MPa,

$n_1 = 50,000$ cycles, $R = 0.5$, $\sigma_2 = 32$ MPa; $n_2 = 100,000$ cycles, $R = 0$, $\sigma_2 = 30$,

$$\sigma_{\text{max}}^{\text{Master}} = c1 + (\bar{R}_\perp^t - c1) / \exp\left(\frac{\log(N)}{c3}\right)^{c2} \quad \text{with } c1 = 7.1, c2 = 1.34, c3 = 6.05,$$

$$\Psi_{\text{Master}}^t = \frac{\sigma_{2a}}{\bar{R}_\perp^t - \sigma_{2m}} = 0.5 \cdot \sigma_{\text{max}}^{\text{Master}} \cdot (1 - R) / \left[\bar{R}_\perp^t - 0.5 \cdot \sigma_{\text{max}}^{\text{Master}} (1 + R) \right]$$

and after resolution an equation for the determination of a desired $S - N$ curve, inserting R

$$\sigma_{\text{max}} = 2 \cdot \bar{R}_\perp^t \cdot \Psi_{\text{Master}}^t / (\Psi_{\text{Master}}^t - R + R \cdot \Psi_{\text{Master}}^t + 1), \quad 0 < R < 1.$$

*Estimation of fracture cycles N at $D_i = n_i / N_i = 100\%$.

$$\sigma_{R=0.5} = 2 \cdot \bar{R}_\perp^t \cdot \Psi_{\text{Master}}^t / (\Psi_{\text{Master}}^t - 0.5 + 0.5 \cdot \Psi_{\text{Master}}^t + 1) = \sigma_2 \rightarrow N_1 = 4.6 \cdot 10^5,$$

$$\sigma_{R=0} = 2 \cdot \bar{R}_\perp^t \cdot \Psi_{\text{Master}}^t / (\Psi_{\text{Master}}^t - 0 + 0 \cdot \Psi_{\text{Master}}^t + 1) = \sigma_2 \rightarrow N_2 = 1.7 \cdot 10^6.$$

*Summing up the micro-damage portions \rightarrow total $D_i = \Sigma n_i / N_i = 0.17 < 1 = 100\%$.

*From experience with the $S - N$ scatter $\rightarrow RF_{\text{Life}}$ should be > 5 (termed 'Relative Miner')

$$RF_{\text{Life}} = 100\% / \text{total } D = 1 / 0.17 = 6 > 5!$$

7. Conclusions on the Author's FMC and SFCs Derived and Novel Ideas Elaborated

7.1. Conclusions on the Author's FMC-based SFCs, preferably UD materials

- The FMC is a material symmetry-driven, invariant-linked basis to optimally generate SFCs like 'Mises', who was the author's inspiring invariant idol.

- The invariant-based 3D-SFC set (*transfer between coordinate systems is automatically given*) and is physically-based due to the choice of solid-behavior associated invariants together with material-symmetry. If the material element experiences a volume change, a shape change and friction, then, a successful demonstration of the advantageous use of the 'physics-based' invariants could be given.

- FMC-based 'modal' SFCs are simple but describe physics of each separately mapped failure mechanism of different material families pretty well [1, 23]. They deliver a combined formulation of independent modal failure modes, without facing the shortcomings of 'global' SFC formulations, which mathematically combine *in-dependent* failure modes.

- The determination of model parameters is to perform by mapping test data in each pure failure domain, and of the interaction exponent m by mapping the transition zone between the modes. A good guess is $m = 2.6$ for all mode transition domains and all material families.

- The experience of the author proves: Similarly behaving materials possess the same shape of a fracture body and the same F can be used.

- The use of the entity Eff excellently supports 'understanding the multi-axial strength capacity of materials.' 3D-compression stress states have a higher load-bearing capacity, but the value of Eff nevertheless remains at 100%. This has nothing to do with an increase of a (uniaxial) technical strength R which is the result of a Standard-fixed, welcomed common agreement that offers the chance to compare material properties! The following test result of a concrete impressively shows how a slight hydrostatic pressure of 6 MPa increases the *strength capacity* in the longitudinal axis from 160 MPa up to 230MPa – 6 MPa = 224 MPa. Therefore, use the benefit of 3D-SFCs

$$\sigma_{\text{fracture}} = (\sigma_I, \sigma_{II}, \sigma_{III})_{\text{fracture}}^T : (-160, 0, 0)^T \Rightarrow (-224-6, -6, -6)^T.$$

Both the Eff s are 1 = 100% for $(-160, 0, 0)^T$ and $(-224-6, -6, -6)^T$ in [1]! This can be transferred to the quasi-isotropic plane of the UD-material $\sigma_2 - \sigma_3$.

- The size of each Eff^{mode} informs the designing engineer about the failure importance of a mode.

- Clear equivalent stresses can be calculated for the presented modal SFCs. In this context, one should remember: Unfortunately, in general, equivalent stresses are differently defined which produces confusion and does not give a hint which mode is the critical one for the redesign.

- A usual SFC just describes a 1-fold occurring failure mode or mechanism! A multi-fold occurrence of the same failure mode with its joint probabilistic failure effect must be additionally considered in each formulated modal SFC or global SFC.

Question: Which of the popular SFCs takes care of this effect?

- Fracture angles can be determined with the scalar FMC-SFCs – after Mohr–Coulomb transformation — for each mode, but due to the scatter experienced in tests, the additional value of a predicted fracture angle value most often seems to be a little questionable.

- A 3D-SFC can be validated, principally, by 3D test data sets, only. If just 2D-test data is available, then the 2D-reduced 3D-SFC is applied. This means that the necessary 3D-mapping quality is not fully proven.

- Effective lamina strengths depend on ply-'thinness' and stress rate. Beyond IFF the embedded ply, strain-controlled by the vicinity, still contributes to the strength and stiffness capacity.

- Switching between material families generally improves material understanding.

7.2. Elaborated novel ideas

• Considering Material symmetry: There seems to exist a ‘generic’ number for material families, namely 2 for isotropic and 5 for transversely-isotropic materials.

• Direct use of the measurable, physically clear friction value α in the SFC formulation instead of using fictitious friction model parameter. This matches with the engineer’s thinking in physical properties. A good guess for isotropic and UD materials is $\alpha = 0.2$.

• Automatic determination of the Constant Fatigue Life curve could be presented which allows one a fatigue life estimation on a minimum amount of test effort.

• Isotropic material-inherent 120°-symmetry, known for tested compressed concrete failure bodies and displayed in the octahedral stress plane, could be demonstrated for tested ductile isotropic materials (metals, tensile), too, using the

Extended Mises Model 3 · $J_2 \cdot \Theta + c_{12} \cdot I_1^2 = (\bar{R}^t)^2 \cdot c_\tau$ with $\Theta = 120^\circ$ -considering
non-circularity parameter, c_{12} shape parameter, c_τ size parameter, \bar{R}^t normalization strength.

• Beside the SFCs for FF and IFF of ‘dense’ UD-materials an IFF2-SFC for a ‘porous’ UD- material was derived.

• Derivation of a tension-caused porosity-considering flow curve of a plastic-behaving ductile isotropic material (metal, polymer)

$$\Rightarrow \sigma_{\text{eq}}^{\text{ExtMises}} = \frac{F}{A} / (1 + 2 \cdot \rho / a) \cdot \ln(1 + a / 2 \cdot \rho) / \sqrt{3 \cdot J_2 \cdot 1 + c_{12} \cdot I_1^2}, \text{ valid } \bar{R}^t < \bar{R}_{\text{odc}}$$

(\bar{R}_{odc} set as strain-driven Design Limit at ‘Onset-of-ductile cracking’ = onset coagulation of voids)

using Bridgman correction of the tensile rod test, Lorrek–Hill’s approach for the neck curvature development a / ρ , the continuously measured constriction of the thickness diameter $2a$ as function of force F , true area A and a *comparison of coefficients* between the ‘FMC-based Extended Mises model’ and the ‘Gurson model’ in order to capture the load-driven increasing porosity f by $c_{12}(f)$, with f modeled as an exponential function [1].

• Mechanics building could be ‘smoothed’: (1) Beside SY also NY exists and could be firstly modelled. (2) For an ideally homogeneous situation in front of the crack tip of a brittle material, beside $K_{Ic} \equiv K_{cr}^c$ a with K_{cr}^c a second critical stress intensity factor or fracture toughness was identified, where the fracture plane growth further in its plane which means that the original crack plane remains stable under further loading [1].

It’s one thing to have an idea, here the FMC, but it’s another to make it fly.

Didn’t the strict application of failure modes, material symmetry and invariants help to make the mechanical building clearer and thereby simpler?

Acknowledgement. The single authored, non-funded FMC and the later compiled Life-Work include the works: *Idea finding, *idea exploitation to generate the FMC-theory, *text writing, *extensive numerical analyses with difficult visualizations of results like failure bodies using the program MathCad, *typing of formulas. All these works have been performed by the author himself. Nevertheless, many thanks are given to those who believed in my general FMC work [W. Becker] and – in spite of my critical comments, being honest - it includes the ‘tough’ organizers within the performance of WWFE-I and –II on UD materials from 1999 through 2013, especially Sam Kaddour.

REFERENCES

1. R. Cuntze, "Life-Work Cuntze - a compilation," > 750 pages, Draft December 2022, permanent downloading address from January 2023 on: Carbon Connected | Prof. Ralf Cuntze (carbon-connected.de)
2. R. Cuntze, "Application of 3D-strength criteria, based on the so-called "Failure Mode Concept", to multi-axial test data of sandwich foam, concrete, epoxy, CFRP-UD lamina, CMC-Fabric Lamina," ICCE/5, Las Vegas, July 1998 (presentation).
3. R. Cuntze, "Failure conditions for isotropic materials, unidirectional composites, woven fabrics - their visualization and links," <https://www.ndt.net › cdc2006 › papers › cuntze>, PDF.
4. R. M. Christensen, "The numbers of elastic properties and failure parameters for fiber composites," Transactions of the ASME, **120**, 110-113 (1998).
5. S. W. Tsai and E. M., "A general theory of strength for an-isotropic materials," J. Comp. Mater., **5**, 58-80 (1971).
6. R. Cuntze, R. Deska, B. Szelinski, R. Jeltsch-Fricker, S. Meckbach, D. Huybrechts, J. Kopp, L. Kroll, S. Gollwitzer, and R. Rackwitz, New Fracture Criteria — Hashin-Puck Action Plane Criteria — and Strength Design Verifications' for Unidirectional FRPs Subjected to Multi-axial States of Stress – Model Development and Experiments. [in German] VDI-Fortschrittbericht, Reihe **5**, Nr. 506 (1997).
7. German Guideline, Sheet 3, Development of Fibre-Reinforced Plastic Components, Analysis, Beuth-Verlag, 2006 (in German and English, author was convenor and co-author).
8. R. Cuntze, "Comparison between experimental and theoretical results using cuntze's failure mode concept model for composites under tri-axial loadings – Part B of the WWFE-II.," J. Compos. Mater., **47**, 893-924 (2013).
9. A. Puck, Festigkeitsanalyse von Faser-Matrix-Laminaten - Modelle für die Praxis, München, Carl Hanser Verlag (1996).
10. R. Cuntze, "Efficient 3D and 2D failure conditions for UD laminae and their application within the verification of the laminate design," Compos. Sci. and Technol., **66**, 1081-1096 (2006).
11. R. Cuntze, "Strength failure conditions of the various structural materials: is there some common basis existing?," SDHM, **74**, No.1, 1-19 (2008).
12. R. Cuntze, "The predictive capability of failure mode concept-based strength conditions for laminates composed of UD laminae under static tri-axial stress states, WFE-II, Part A," J. Compos. Mater., **46**, 2563-2594 (2012).
13. H. Awaji and S. Sato, "A Statistical theory for the fracture of brittle solids under multiaxial stresses," Int. J. Fracture, **14**, 13-16 (1978).
14. J. P. Boehler, "Introduction to the invariant formulation of anisotropic constitutive equations," In: J. P. Boehler (Ed.) Applications of Tensor Functions in Solid Mechanics", CISM Course No. 292, Springer-Verlag (1987). In addition a personal note from J. Boehler on UD-invariants which were later applied by the author in his FMC.
15. E. Petersen, R. Cuntze, and C. Huehne, "Experimental determination of material parameters in Cuntze's failure-mode-concept-based UD strength failure conditions", Compos. Sci. and Technol., **134**, 12-25 (2016).
16. R. Cuntze, "The Predictive capability of failure mode concept-based strength criteria for multidirectional laminates, Part B," Compos. Sci. and Technol., **63**, 487-516 (2004).
17. R. Cuntze, "Fracture failure bodies of porous concrete (foam-like), normal concrete, ultra-high-performance-concrete and of the lamella — generated on basis of Cuntze's failure-mode-concept (FMC)," NWC2017, June 11-14, NAFEMS, Stockholm (2017).
18. M. J. Hinton, A. S. Kaddour, and P. D. Soden, "A comparison of the predictive capabilities of current failure theories for composite laminates, judged against experimental evidence," Compos. Sci. and Technol., **62**, 1725-97 (2002).
19. A. S. Kaddour and M. Hinton, "Maturity of 3D failure criteria for fiber-reinforced composites: Comparison between theories and experiments, Part B of WWFE-II," J. Compos. Mater. **47**, Nos. 6-7, 925-966 (2013).
20. R. Birch, "The Effect of pressure upon the elastic parameters of isotropic solids, according to Murnaghan's theory of finite strains," J. Appl. Physics, **9**, No. 4, 279-288 (1938).

21. M. Kawai, "A phenomenological model for off-axis fatigue behaviour of uni-directional polymer matrix composites under different stress ratios," *Compos., Part A*, **35**, 955-963 (2004).
22. Hahne C, *Zur Festigkeitsbewertung von Strukturbauteilen aus Kohlenstofffaser-Kunststoff-Verbunden unter PKW-Betriebslasten*, Shaker Verlag, Dissertation 2015, TU-Darmstadt, Schriftenreihe Konstruktiver Leichtbau mit Faser-Kunststoff-Verbunden, Herausgeber Prof. Dr.-Ing Helmut Schürmann (2015).
23. A. Puck and H. Schuermann, "Failure analysis of FRP laminates by means of physically based phenomenological models," *Compos. Sci. and Technol.*, **62**, 1633-1662 (2002).